CHARACTERIZATION AND MODELING OF THE STEADY STATE AND TRANSIENTS OF MODULATED HOLLOW CATHODE DISCHARGES OF NITRIC OXIDE

M. Castillo, V. J. Herrero, I. Tanarro*
Instituto de Estructura de la Materia (CSIC), Serrano 123, 28006 Madrid, Spain
*Corresponding author. Fax: +34.91.5855184; e-mail: itanarro@iem.cfmac.csic.es

ABSTRACT

This work describes a systematic experimental study and kinetic modelling of the steady state and the transients associated with the turn on and off of a NO hollow cathode discharge. The local charge density and mean electron energy have been determined with a double Langmuir probe. Time-resolved Fourier transform infrared spectroscopy and electron bombardment quadrupole mass spectrometry with ionisation by electron impact have been used to measure the gas temperature and the concentrations of the stable molecules present in the discharge: the precursor, NO, the major products, N_2, O_2, and the minor species NO_2 and N_2O. Emission spectroscopy has been employed to study the time behaviour of the very reactive nitrogen and oxygen atoms. A model based on a reduced set of kinetic equations including electron dissociation, gas-phase reactions, and gas-surface processes gives a global account of the measured data. From the time resolved results, electron impact dissociation rate constants for some of the involved species under the conditions of the experiment are estimated. The present model is compared with that obtained in previous works on N_2O plasmas.

1. Introduction

The non-equilibrium kinetics of low pressure plasmas of nitrogen oxides, N_2, O_2, and their mixtures, is presently attracting attention in modern plasma physics research [1-7] due to its relevance in different fields, ranging from plasma based technologies to the study of the Earth ionosphere and the interstellar space. In particular, the study of the volume and surface kinetics of the nitrogen and oxygen atoms appearing in this kind of plasmas after the dissociation processes produced by electron impact, and the role of the very active NO molecules, may be decisive to unravel the detailed mechanisms governing the behaviour of plasma reactors employed in chemical vapour deposition of thin films [8], surface treatments, vacuum vessel cleaning [9] and air pollution control [10-13], or even to explain the formation of NO and NO_2 molecules in the surface of space vehicles in the upper atmosphere. Homogeneous reactions involving these species are also responsible for the predominance of O_2^+ and NO^+ ions in the low density plasma originated in the E shell of the ionosphere by extreme UV and soft X radiation and by cosmic rays [14].

Very popular kinds of low pressure laboratory plasmas are those produced in pulsed and continuous glow discharges, and particularly, those obtained in hollow cathode reactors [15-17]. Hollow cathode cells provide a good geometrical resolution with an abrupt transition between the different zones of the discharge, resulting in a nearly total confinement of the plasma in the negative glow, and thus facilitate the determination of the boundary conditions in the kinetic modelling and the use of diagnostic techniques for the investigation of basic plasma parameters. Furthermore, the negative glow can be extended geometrically in a nearly undefined length with the suitable selection of the cathode dimensions, providing one of the best available plasma configurations in order to study atomic and molecular transient species which appear at very low concentrations [18].

In previous works, the authors have studied extensively the properties of plasmas produced in DC hollow cathode discharges of N_2O [6] under different physical conditions (gas pressure, flow rate, electric current…), verifying the formation of the major stable products NO, N_2 and O_2, which had been already observed in former works on N_2O RF glow discharges [19,20], but observing also the appearance of small but significant quantities of NO_2, not reported previously in the bibliography on N_2O discharges. In order to explain the observed data, a kinetic model was developed, including the most relevant physical and chemical processes involving electrons and neutral species in a set of coupled, time-dependent, linear differential equations. Most reaction rate constants were taken from published databases, especially those for homogeneous reactions among neutrals; but a few of them, notably those for electron impact dissociation and heterogeneous processes, which are very dependent on the particular experimental conditions (detailed electron energy distribution or wall properties) and are in general not available, had to be estimated.

In order to estimate individual rate constants from experimental data, the time evolution of the different species during the ignition and the extinction of the discharge has proven much more useful than the steady state results [21]. Consequently, the time dependence of the concentration of the precursor in the fundamental and in some vibrational excited levels, as well as that of all the molecular products of the N_2O plasma, were experimentally studied at different discharge modulation frequencies and different time scales, for the first time [22,23].

The convenience of using time resolved techniques to unravel the complex mechanisms relevant for the plasma chemistry has been stated soundly in the literature

[1,24-26]. Furthermore, the absolute calibration of time scales is usually easier and much more direct than that of the magnitudes needed for the determination of absolute concentrations in the stationary plasma, like electron density and ion currents, light emission, or peaks in the mass spectra.

In this work, DC and square wave modulated NO plasmas have been generated and studied in a hollow cathode reactor similar to that used previously in our laboratory for the investigation of N_2O plasmas. Many of the elementary processes present in a NO discharge should be basically the same as those involved in a N_2O plasma, where NO, N_2 and O_2 are generated as major products, and the present study should help to verify the kinetic model and the rate constant values suggested in former works. In addition, the use of NO instead of N_2O as the discharge precursor, should provide new and valuable information for a better understanding of the physical chemistry of nitrogen oxide cold plasmas, since the first dissociation and reaction steps are not the same, and the time evolution and relative concentrations of the stable products and of atomic nitrogen and oxygen are expected to differ markedly. Besides, the knowledge of the specific dissociation mechanisms of NO is presently a subject of great interest, directly related with the control by means of plasma techniques of the emissions to the atmosphere of this toxic species and its derivative, the more stable and even more toxic NO_2 molecule, both formed in diesel engines and other high temperature burning processes.

In order to achieve a characterization as complete as possible of the nitric oxide plasma, a combination of experimental techniques has been used. Electron energies and number densities were determined with a double Langmuir probe. NO, N_2 and O_2 were detected with a quadrupole mass spectrometer (QMS). FTIR spectroscopy was used for monitoring once more the precursor, NO, and the nitrogen oxides N_2O and NO_2 produced in the discharge. Atomic nitrogen and oxygen were detected by means of dispersive emission spectroscopy in the visible region. The measurements were carried out in the stationary state of the DC discharges and with time resolution in the modulated ones, for different gas flows through the discharge cell as well as for distinct values of both, total pressure and discharge power. The experimental results are discussed and compared to the predictions of the kinetic modeling and to previous works on plasmas of N_2O.

2. Experimental details

2.1. Hollow cathode discharge cell

The experimental measurements of the present work were carried out with the hollow cathode discharge cell mentioned in the previous section, which was specially designed in our laboratory for both absorption and emission spectroscopy, as well as for mass spectrometry and Langmuir probe measurements, with just the proper selection of the different kinds of assemblies and windows to be employed at its two ends. Its description can be found elsewhere [6,22]. Briefly, the discharge cell has a symmetrical electrode geometry and consists of a cylindrical hollow stainless steel cathode, 90 mm long and with a 16 mm inner diameter, and two circular copper anodes, each one of them placed at one end of the cathode at a distance of 25 mm from it, and supported by anode holders made of Pyrex and stainless steel. The discharge is fed by a 2000 V, 150 mA, square-wave modulated source, operative between 0 and 200 Hz. The electrodes are refrigerated by water.

The discharge is sustained in a continuous and adjustable flow of NO, evacuated by a rotary pump and a liquid nitrogen trap. In order to neutralize NO at the gas exhaust,

a double trap containing a saturated solution of NaOH in water is installed after the rotary pump. The gas flow is controlled by a needle valve and measured by means of a calibrated rotameter placed at the entrance of the cell. The gas pressure in the cell is controlled with a regulating valve located between the cell and the vacuum system and is measured by means of a capacitance manometer placed just at the exit of the cell.

2.2. Langmuir probe

Charge density and electron temperature were measured by means of a double Langmuir probe built in our laboratory. It should be noted that electric probes inserted in the plasma lead to disturbances that may modify the measurement conditions and may introduce uncertainties in the results [27]. In this sense, double Langmuir probes first developed by Johnson and Malter [28] are very suited in order to minimize the perturbation effects, since they eliminate potentials higher than that of the plasma [29].

The Langmuir probe consisted of two parallel, 10 mm length, 65 μm radius tungsten wires protruding from two capillary tubes of glass sealed at the end. The separation between the wires was 1mm. It operated with a floating AC signal of 50 Hz, ±70 V. The V-I characteristic curves were recorded on a digital oscilloscope working in the X-Y mode, connected through isolating electrical probes. The probe was mounted on a movable vacuum flange, which allowed a radial displacement of ±1 cm and some 10 cm in the axial direction. In this way, ion density and electron temperature could be tested in different positions of the discharge: along the cathode inner diameter, and along the symmetry axis of the cell, inside and outside the cathode region. Similarly to previous studies on N_2O discharges [6,22,23], the charge density was observed to be nearly constant in the negative glow region and to decrease abruptly outside it; its value depending on gas pressure and varying linearly with electrical current up to approximately 10^{11} (±10%) cm^{-3} for 100 mA. The negative glow region extended axially along the whole cathode length and, radially, until the cathode sheath at a distance of ~1–2 mm from the cathode wall, depending on pressure. The circular limit between the cathode sheath and the luminescent negative glow can be clearly distinguished at a glance too. The electron temperature was constant inside the negative glow, reaching a value of 35000 (±15%) K for the gas pressures employed in the present work, equal to that obtained in previous works on N_2O discharges within the experimental uncertainties, although its value was observed to grow with decreasing pressure (below 0.1 mbar). The uncertainty in electron density given above was estimated from the deviation of the experimental values from their linear dependence with discharge current. The uncertainty in electron temperature is the standard deviation of eight measurements taken under the same experimental conditions.

Electron density was determined from probe data by assuming a collision free probe sheath and an orbital motion limited (OML) range (*i.e.*, mean free path, $\lambda >>$ Debye length, $\lambda_D >>$ probe radius, r_p). Under the present discharge conditions, with NO pressures between 0.1 and 0.7 mbar and with the electron temperature and density data given above, the values $\lambda \sim (600–85)$ μm, $\lambda_D \geq 40$ μm and $r_p = 60$ μm do not justify these assumptions. However, it is generally accepted [19,27,29] that even for collisional sheaths, Langmuir probe results are reliable, provided that λ, λ_D and r_p are comparable. In our case, $\varepsilon = r_p/\lambda_D \leq 1.6$ and the use of the Laframboise's [30] theory in the OML region of probe operation is justified [31]. Nevertheless, with these assumptions, and taken into account the influence of possible disturbances in the plasma caused by the probe, errors in the

electron densities may be higher (~up to 25-30%) than those deduced from the experimental uncertainties commented on in the previous paragraph.

Concerning the electron energy distribution function (EDF), it is well known that, for low pressure plasmas, the Druyvesteyn distribution gives often a better approximation than the Maxwellian one, or even that a superposition of several nearly Maxwellian distribution functions with different temperatures may be found [27,32]. As stated by Clements [33], single probes, which sample the complete EDF, provide direct data about its possible deviations from the Maxwellian shape. On the contrary, only the high-energy tail of the EDF is sampled in double probes. In this case, a temperature to the electrons is ascribed, even though they are far from being thermalized. In the present work, attempts to use a single Langmuir probe failed because a secondary glow appeared in it; and, with the double probe, the above mentioned temperature of 35000 K (±15%) was obtained, corresponding to an electron mean energy of 3.0±0.5 eV by assuming a Maxwellian distribution.

In order to verify the speed of appearance and extinction of the charge density following the square wave modulation of the discharge, the temporal response in electrical current of the Langmuir probe was recorded for a constant value of the floating potential applied between the two wires during a modulation period. Once the discharge was turned on or off, the current intensity reached a constant value or disappeared respectively in less than 10 μs. This is in good agreement with other estimates found in the literature [34] and indicates that, for the time scales of the present work, the appearance of ions and electrons may be assumed to be instantaneous.

2.3. Mass spectrometry

The detection of the precursor, NO, and of the most abundant stable species generated in the discharge, N_2 and O_2, was done by means of an electron bombardment QMS, Balzers QMG112, with a Faraday cup as the charge collector. The quadrupole vacuum chamber was evacuated by means of a 300 l/s oil pump provided with a liquid nitrogen trap and backed by a 35 m^3/h rotary pump. A pressure of 7×10^{-7} mbar was achieved in the isolated chamber. A gate valve and an aperture with a diameter of 50 μm located at the end of the cell established the communication between the discharge cell and the quadrupole vacuum chamber. This diaphragm was done by means of electro-erosion on a 100 μm thickness stainless-steel sheet, following the method described in [35]. The pressure in the mass spectrometer chamber, under the usual operating conditions in the discharge cell (up to 1 mbar), never exceeded 5.10^{-6} mbar. In order to obtain absolute concentration data, the sensitivity of the spectrometer to NO, N_2 and O_2 was calibrated before and after each set of plasma measurements, by introducing these pure gases separately in the cell at various known pressures and measuring the QMS signal. The calibration signals were proportional to the cell pressures for the various gases in all the cases, with linear regression coefficients larger than 0.999. The reproducibility of the calibrations was very good, so that even the differences in calibrations taken with a time interval of one month were smaller than 10%. The effective time resolution of the quadrupole mass spectrometer system is determined by the gas residence time in the quadrupole vacuum chamber, which depends on its volume (3.5 l) and the pumping speed. In the present case this value is 12 ms.

2.4. FTIR absorption spectroscopy

Minor stable species of the NO discharge, such as N_2O and NO_2, could not be detected by mass spectrometry due to a lack of sensitivity and because of overlapping of some of the most intense mass peaks of the respective fragmentation patterns. Therefore, these infrared active molecules were detected by Fourier transform infrared (FTIR) absorption spectroscopy (N_2O: ν_3 band centered at 2223.7 cm^{-1}; NO_2: ν_3 band centered at 1616.7 cm^{-1}. The band of NO at 1876 cm^{-1} was also detected) [36].

For the FTIR measurements of the nitrogen oxides concentration, a Bruker IFS66 spectrometer was used in the rapid-scan option of its movable mirror, with a deuterated triglycine sulphate (DTGS) detector. The spectral range of this apparatus is 400 - 7000 cm^{-1}. It allows dry air purging of the optical bench, in order to prevent water vapor absorptions. The maximum experimental resolution attainable (0.1 cm^{-1}) is not sufficient to resolve the individual vib-rotational lines of the N_xO_y species.

In order to determine the gas temperature and the N_xO_y species concentrations, a comparison with the simulated infrared spectra of NO, N_2O and NO_2 was done by means of the spectroscopic data of wave numbers and absorption coefficients of the HITRAN database [37]. These data have been treated by taking into account optical path length effects (Lambert-Beer law), and assuming a gaussian line shape for the natural line profiles, in order to simulate the transmittance spectra. An apodization function of the Blackman-Harris type with three terms, which supplies also a near gaussian instrumental line shape, has been used in the FTIR spectrometer [38]. The simulated spectra have been convoluted with this instrumental line shape and have been converted into absorbance spectra for a direct comparison with the experimental results. From these data, it could be established that the temperature of the discharge, related with the rotational population and the translation distribution functions, did not increase much with respect to that of the ambient (with an experimental uncertainty of 50 K) in agreement with previous results from hollow cathode discharges of other species [22,24]. The experimental uncertainties of the absolute concentration data, coming both from the noise in the transmittance signals and from the numerical fitting of the molecular bands, performed as explained above, were approximately ~10-25%, depending on the species and the concentration values.

For the time resolved measurements, the minimum time required to perform a complete interferogram with the low spectral resolution of 40 cm^{-1} used for this purpose and a mirror speed of 0.3 $cm.s^{-1}$ is ~ 42 ms, and taking into account the time interval between the end of a scan and the beginning of the following one, a time resolution of 100 ms was achieved. This resolution is enough to measure the transient phenomena of interest in the present work with a suitable level of detail.

2.5. Visible emission spectroscopy

Visible emissions of electronically excited species were recorded by means of a dispersive set-up consisting of a Monochromator Oriel 77200 with an holographic grating of 1200 lines/mm blazed at 500 nm and slits of 100 μm, and a photomultiplier RCA 4526/M3 working analogically. The spectral range was 300-850 nm, with a spectral resolution of 1 nm. The time resolution was limited to 5 ms by the electronic amplifier and pulse integration circuit of the photo-multiplier.

3. Experimental results

Figure 1 shows the dissociation of the NO precursor in the hollow cathode discharge and the concentrations of N_2 and O_2 obtained for different values of the electrical current,

expressed in molar fractions, for a constant pressure and gas flow rate. The electron densities obtained with the double Langmuir probe for the different current values are also shown. Roughly, one molecule of N_2 and another one of O_2 are produced for every two NO molecules dissociated, and the total gas pressure remains nearly constant, since the triatomic nitrogen oxides appear only in small amounts, as will be seen in figure 2. In figure 1, the theoretical concentrations of the three diatomic species simulated with the present kinetic model (see below) are also displayed. In the model, the experimental values of the electron densities are taken explicitly into account. In general, the concentration of the different species depends strongly on the particular experimental conditions employed in each case, such as electron density, plasma volume, wall conditions and residence time.

In figure 2 the experimental results obtained by means of mass spectrometry and FTIR spectroscopy for the stationary absolute concentrations of the stable species involved in DC nitric oxide discharges are shown, at constant pressure and electrical current and for different gas flow rates. In this figure, the decrease in concentration of the precursor and the growth of the mayor products N_2 and O_2 with decreasing flow rates and increasing residence times, as recorded by the mass spectrometer, are shown. Besides, the minor but appreciable concentrations of the tri-atomic nitrogen oxides, N_2O and NO_2 are shown, as observed by means of FTIR spectroscopy. In the same figure, these experimental results are compared with the model simulations. The model, which is an improved version of that developed for N_2O plasmas [22], includes the reactions shown in table 1 and will be described in the next section.

Figure 3 shows the time evolution of the NO, N_2 and O_2 concentrations when the discharge is turned on and off periodically at a frequency of 0.1 Hz, as measured with the mass spectrometer and reproduced with the kinetic model. The time-resolved data are in general much more sensitive to the values of the model rate constants that the steady state results and can be of great help for the estimate of rate constants not available in the literature, as discussed below. The time evolution of the major species after the switching off of the discharge depends only on the gas flow rate and gives the residence time in the reactor. The value thus obtained, which is a key parameter of the model, is more precise than that determined from rotameter flow measurements or from conductance calculations

The highly reactive nitrogen and oxygen atoms, only present as reaction intermediates in small amounts, are confined to the plasma region and cannot be detected with the QMS. They are however easily observed, even with time resolution, in the visible emission spectrum of the discharge. In fact, the time evolution of the atomic emission spectra provides a most valuable information for the estimate of electron impact dissociation rate constants, which can depend appreciably on the particular set-up used and are in general difficult to determine. Figure 4 shows the time dependence of the fluorescence signals of N_2, N and O when the discharge is turned on, together with the corresponding model simulations for N_2, N and O in their fundamental states. Note the different behaviour of the three species considered and the good agreement between experimental and theoretical data. After switching off the discharge, the emission goes down suddenly, following the fast deexcitation of electronically excited levels, with natural lifetimes of only several nanoseconds. The time evolution of N_2 when the discharge is on, observed with the transitions whose band-heads are found at 6317 Å and at 3371 Å, coincides with that observed by mass spectrometry at the same experimental conditions, thus indicating that the fluorescence process is really very quick in this time scale and that the fraction of excited molecules is proportional to the total amount of N_2 molecules being formed. In order to study the N fluorescence, the unresolved signal of

the lines at 8210.7 and 8216.3 Å, corresponding to $3s^4P(3/2)$-$3p^4P^o(3/2)$ and $3s^4P(5/2)$-$3p^4P^o(5/2)$ transitions respectively, was employed. Similarly, for atomic oxygen, the unresolved triplet at 6156.0, 6156.8, 6158.2 Å, of transitions between the $3p^5P$ and $4d^5D^o$ multiplets, was used [39].

Visible emissions of some of the ions like N^+, O^+ and N_2^+ were identified in the spectra, but with very small intensities as compared with those from neutrals. Throughout the present work ions have been assumed to play a comparatively minor role in the global discharge chemistry and have not been taken into account (see comment below).

4. **Kinetic model**

The kinetic model used here and summarized in table 1 is based on the numerical integration of a system of coupled differential equations accounting for the time evolution of the plasma species, and is an improved extension of that used previously by the authors for the characterization of N_2O discharges [6,22].

After switching on the discharge, NO is dissociated by electron impact (reaction D1 in table 1) and its concentration decreases markedly; the N and O atoms formed recombine at the reactor walls (reactions W1 – W3) and react in the gas phase (reaction G1). These reactions are responsible for most of the O_2 and N_2 build up, and cause also an additional and appreciable reduction in the NO concentration. Reaction W4 leading to NO formation in the wall compensates to a small extent the loss of NO by electron impact and gas phase reactions.

Reactions G2 – G4 and W5, W6 account for the appearance of N_2O, as well as for the formation and disappearance of NO_2 in gas phase processes and in heterogeneous reactions. These tri-atomic oxides are minor stable compounds of the NO discharge. Reactions G4 and W6, which explain the formation of N_2O, were not included in our previous modelling of N_2O plasmas, since they were not significant in comparison with the continuous supply of fresh N_2O, which was then the discharge precursor; nevertheless these reactions are necessary here in order to explain the small but noticeable concentration of this species present in the NO discharge.

Reactions D2-D8 correspond to the dissociation of the stable products by electronic impact. Two channels should be taken into account for the dissociation of O_2; the first one gives rise to two oxygen atoms in their fundamental state $O(^3P)$, and the second one produces an oxygen atom in the fundamental state plus another one in the metastable $O(^1D)$ state, whose natural deexcitation lifetime is 150 s [40]. Once formed, $O(^1D)$ reacts very actively with all the nitrogen oxides, NO, N_2O and NO_2 (reactions G5-G8), contributing very efficiently to their disappearance; or decays by quenching with the major species (reactions Q1 – Q3) or by collisions with the wall (reaction W7). Figure 5 shows a semi-logarithmic plot of the predicted temporal evolutions of all the atomic and molecular species considered in the kinetic model, in a 0.6 mbar, 2sccm, 40 mA, square wave modulated NO discharge.

The good agreement between the model simulations and the measurements was already mentioned in the presentation of the experimental results (Figs 3 and 4). It should be noted here that the time evolution of the N and O atomic species (middle and lower panel of Fig 4) was monitored by recording the fluorescence from electronically excited states of these atoms. For the comparison of the fluorescence signals with the model calculations, which yield the total concentration of N and O, it has been assumed that following the processes of electronic excitation by electron impact, the subsequent radiative deexcitation of the atoms in the plasma is very fast and, as a consequence, the

fraction of the excited atoms responsible for the fluorescence is proportional to the total amount of the corresponding atomic species. In the case of oxygen, it is further assumed that the fluorescence signals correspond to excitations of the fundamental state ($2p^4\ ^3P$) of oxygen, since, as seen in figure 5, the metastable O ($2p^4\ ^1D$), which appears as a secondary dissociation product of O_2 and is the most reactive species in the plasma, is only present in a concentration much smaller than that of O($3p^4\ ^3P$) during the NO discharge. Besides, selection rules for electron impact excitation to the upper level of the radiative transition preclude absolutely the change in the quantum spin number $\Delta S = 2$ needed for the excitation of the O(^1D) level to the O($4d\ ^5D^o$) fluorescing state. The variation $\Delta S = 1$, necessary for the excitation from the fundamental O($3p^4\ ^3P$) state to the excited O($4d\ ^5D^o$) one, is also forbidden, but the corresponding selection rule is not so strict and in fact, this kind of transitions has been frequently observed in the excitation of atoms and molecules by impact with low energy electrons [41]. Contributions to atomic fluorescence signals of N and O coming from dissociative excitation of N_2 and O_2 were not taken into account in the model. In spite of the much higher concentrations of N_2 and O_2, as compared with those of N and O in the plasma, the rate constants for dissociative excitation of N_2 and O_2 are expected to be orders of magnitude lower, given the high threshold energies (21.6 and 17.9 eV, instead of the 11.8 and 12.7 eV needed to excite the N and O atoms from their ground state) [40]. This assumption is confirmed by the time evolution of the fluorescence signals (see figure 4). The appearance of N_2/O_2 in the plasma should be the rate limiting step for their dissociative excitation. In the case of N_2, this evolution is depicted in the upper panel of figure 4. As can be seen, the evolution of this molecular species in the plasma is much slower than that of the atomic fluorescence of N. Data from mass spectrometric measurements of N_2 and O_2 corroborate these results, and the time resolved atomic fluorescence data are well reproduced by the model calculations without considering dissociative excitation.

The rate constant values for the different processes are listed in the second column of table 1. The third column shows the sources of these rate constants. For homogeneous gas phase reactions the NIST and NASA Chemical Databases [42,43] have been preferentially used. As mentioned above, experimental rate constants for electron impact dissociation at low energies are not available in general [32]. They depend strongly on the electron energy distribution in glow discharges, usually approximated by a Maxwellian or a Druyvesteyn distribution, but in general they are not precisely known. In our former work on the kinetics of a N_2O hollow cathode discharge [22] the electron impact dissociation rate constants of NO, N_2O and NO_2, were derived by fitting the model results to the time resolved measurements. After some tests, the former values have been used in the present model without modification because the agreement between experiment and theory obtained here with these dissociation rate constants is good and corroborates the previous estimates. This good accordance is especially encouraging in the case of NO, which was only a minor product in the N_2O discharge. The predictions of the model for two alternative values of the dissociation rate constant of NO are shown in Fig 3 and compared with the experimental results, in order to indicate a conservative upper limit (±20%) in the uncertainty of the value D1 given in table 1. This uncertainty in D1 can also reflect partially the uncertainties in electron density and plasma volume, since in reality it is the product of these three values which is included in the corresponding terms of the differential equations in the model.

The rate constants for the two possible channels in the electron impact dissociation of molecular oxygen have been refined with respect to those of ref [22] by using the expressions in reference [44], where the rate constants are given as a function of the electronic temperature (recall that T_e is measured in the present work). The values

thus obtained for the two channels, assuming 3.0 eV, are higher than those used in the model of the N_2O discharge, but are quite consistent with the present atomic oxygen fluorescence measurements (see Fig. 4), which are more sensitive to the electron impact dissociation of O_2. In Fig 4, the experimental evolution with time of the $O(^3P)$ concentration obtained by fluorescence is compared with those calculated by assuming the rate constants corresponding to 2.8 eV, 3.0 eV and 3.2 eV for the two molecular oxygen dissociation pathways in ref [44]. The sensitivity of the numerical predictions to these changes in energy, lower than the experimental uncertainty deduced from the results of the double Langmuir probe (3.0±0.5 eV), and the comparison with the experimental O concentration, is very encouraging.

The rate constant for the electron impact dissociation of N_2 was considered negligible in our former papers, but an upper limit could be estimated here by fitting the numerical results to the temporal evolution of the nitrogen atom emission, whose behaviour depends strongly of this rate constant, as may be seen in Fig 4. As expected (see for instance [10]) this rate constant is at least one order of magnitude smaller than those for the dissociation of O_2 and the nitrogen oxides.

Summarizing, all the dissociation rate constants of Table I have been obtained by fitting the model and the experimental results, except for the case of O_2 where, it is the electron energy value, measured here, the needed input data in the formulae of Lee et al.[44]. The values (D1,D5-D8) have shown an encouraging consistency with previous works on N_2O discharges.

Sticking, de-excitation and reaction probabilities on the wall surface of the stainless steel cathode (W1-W7) have been taken from references [19,45] W2, [19,20,45] W3, [20] W4, or estimated by fitting the model to the experimental results, when not available in the literature (W5,W6). Nevertheless, these kinds of values may depend for a given material and colliding species, on the specific plasma and wall conditions and the former history of the surfaces exposed to the plasma [46-48] as well as on the ion concentration and energy [49]. On the other hand, when the probability of interaction with the wall is very high ($\gamma \sim 1$), the heterogeneous processes may be limited by diffusion and the rate constants can be estimated essentially from the diffusion coefficients (which depend on pressure and plasma composition) [50,51] and the geometry [52]. In our experiment, the quenching of $O(^1D)$, W7, and the wall adsorption of $O(^3P)$, W1, are assumed to belong to this category, in agreement with the work of Kline and Partlow on N_2O discharges [20], and that allows a reliable estimate of their respective rate constants, which are determinant for the prediction of the concentration of O_2, one of the two major products in the NO plasma. On the other hand, the appearance of the triatomic nitrogen oxides is also attributed here mostly to wall reactions, since the rate constants for the homogeneous processes giving rise to NO_2 and N_2O are too small to account for their experimentally observed concentrations. The rate constants of these two heterogeneous reactions (W5, W6) have been chosen to give a reasonable fit to the observed concentrations of these oxides, but the detailed dependence of the concentrations on the gas flow rate and on the degree of NO dissociation is not well reproduced by the model (see Fig.2)

Ionic species are not expected to play an important role in the overall chemistry of the NO discharges investigated in the present work and they have not been included in the model. Although the cross sections for reactions between charged particles are large [13], the concentration of ions in our plasma is much smaller than that of the neutral species. Langmuir probe measurements give an upper limit of $\approx 10^{+11}$ cm^{-3} for the total ionic concentration. Under these circumstances it has been shown in previous works on

different N_2O glow discharges that the kinetics can be satisfactorily modelled without including the ionic chemistry [6,19,20,22].

The set of coupled differential equations corresponding to the reactions listed in table 1 has been numerically solved . The solution of this set of equations yields the time evolution of the concentrations of each species from the beginning of the discharge to the attainment of the stationary state and from the following extinction of the discharge till the recovery of the original conditions. Besides the five stable molecular compounds NO, N_2, O_2, N_2O and NO_2, the model takes into account the atomic species $O(^3P)$, $O(^1D)$ and N present in the gas phase, and also the O atoms adsorbed on the cathode wall.

For the sake of simplicity, the electron density is assumed to be homogeneous in the plasma volume and negligible outside this region. The plasma volume is located fundamentally inside the cathode, filling the negative glow region. Atomic species, being so reactive, are assumed also to be confined essentially to the plasma volume. On the contrary, the reaction volume for all the molecular species involved in the process is assumed to be the whole cell volume, so the assumption that the stable reagents are well mixed is included implicitly. In order to justify this assumption, the characteristic diffusion time $\tau_d = k_d^{-1}$ of each species in NO, has been estimated [52]. This characteristic time τ_d is of the order of milliseconds, much smaller than the modulation periods of the discharge, and smaller in any case than the residence times ($\tau \approx 0.4 - 3$ s) for all the gas pressures and flow rates studied. Under these conditions, diffusive transport dominates over convection by pumping and the reactor can be considered as effectively well mixed.

In comparison with the time scales relevant for this work, the electron density and energy distributions are assumed to appear and disappear instantaneously upon turning on and off the discharge, in agreement with the present experimental results and some literature studies [17], where transients of some tens of microseconds are reported for the establishment of the stationary state of the electronic distributions in hollow cathode discharges.

5. Summary and Conclusions

In this work the stationary state and the transient processes associated with the ignition and extinction of a low frequency, square wave modulated, hollow cathode discharge of NO until the attainment of the respective stationary states have been studied for the first time. Mass spectrometry and FTIR absorption spectroscopy have been employed for the determination of the absolute concentration of the stable neutral species, emission spectroscopy in the visible region has been used for the observation of atoms through their excited states and a double Langmuir probe has been used for the measurement of the average local electron energy and charge density within the plasma. All these techniques were employed both in continuous and time resolved modes of detection. The temperature of the nitrogen oxides present in the discharge was derived from an analysis of the IR band contours. In accordance with previous studies on glow discharges of nitrogen oxides, N_2 and O_2 are the predominant species in the plasma, formed in this case from the dissociation of NO. In addition, small amounts of N_2O and NO_2 have been clearly identified.

In order to rationalize the collected set of data, a relatively simple chemical kinetics model including a reduced number of reactions is proposed. The model allows a satisfactory simulation of the measured concentrations of the major species present in the discharge (NO, N_2 and O_2), both in the steady state and in the time resolved experiments. Likewise, the observed time evolution of $O(^3P)$ and N atoms is well reproduced within

the model. On the other hand the model accounts only for the order of magnitude of the experimental N_2O and NO_2 concentration, but not for its dependence on the gas flow rate to the discharge cell.

The experimental data on ignition and extinction discharge transients have proven much more sensitive to the rate constant values of individual kinetic processes than those from steady state studies on continuous discharges. In particular, they provide very valuable information on electron impact dissociation rate constants, which are often difficult to obtain. In this respect the present work corroborates the values for the electron impact dissociation rate constants of nitrogen oxides (D1, D5-D8 in table I) derived in a previous study of N_2O hollow cathode discharge. The result is particularly reassuring in the case of NO, which was only a minor product in the N_2O discharge. The time resolved atomic oxygen fluorescence data can be accounted for with a current literature value of the rate constants (D2,D3) for the formation of $O(^3P)$ in the electron impact dissociation of O_2 with electron mean energies of 3 eV; and from the corresponding data on atomic N, an upper limit to the dissociation of molecular nitrogen by electron impact (D4) under our experimental conditions, can be set. Rate constants for heterogeneous formation of N_2O and NO_2 (W5,W6 in table I) are proposed in this work too, in order to explain the appearance of these nitrogen oxides.

The general agreement between calculations and experiment, both time resolved and in the steady state, suggests that the model provides a reasonable global description of the processes performed on the hollow cathode NO discharge.

Acknowledgment

We are indebted to C. Domingo for her help with the FTIR instrument and in the analysis of the bands of nitrogen oxides; and to J. L. Doménech, who wrote the program for the simulation of the spectra. The technical advice of J. M. Castillo, M. A. Moreno and J. Rodríguez have been most valuable for the achievement of the present experiments. The SEUID of Spain (Projects REN2000-1557, PB98-0762-C03-02, FTN2000-0915-C03-03) is gratefully acknowledged for financial support.

Figure Captions

Fig.1 : Experimental (symbols) and calculated (lines) dependences of the molar fractions of the precursor, NO, and the major products, N_2 and O_2, with electrical current. NO pressure: 0.12 mbar; flow rate: 1 sccm. The experimental values of electron density are also shown (right axis). The uncertainties in molar fractions, measured by mass spectrometry, are 10%. The uncertainty in the electron densities may be up to ~ 25%.

Fig. 2 : Experimental and theoretical concentrations of the neutral species found in a steady state 0.75 mbar, 100 mA, NO discharge at different gas flow rates between 1 and 12 sccm. The experimental concentration errors are shown with vertical bars; error bars for the species detected by mass spectrometry (NO, N_2 and O_2) are not larger than the respective symbols. Error bars corresponding to FTIR measurements (N_2O and NO_2) may be seen to reach values up to ~25%.

Fig. 3 : Time resolved mass spectrometric signals of the precursor, NO, and the stable most abundant products, N_2 and O_2, in a 40 mA, square wave 0.1 Hz modulated, 0.6

mbar, 2 sccm, NO discharge. Comparison with the predictions of the model and with those obtained for NO from two alternative values of its dissociation rate constant (see text). The N_2 results have been shifted slightly upwards for clarity of display.

Fig.4: Time resolved emission data in the visible region (continuous lines) showing the evolution of N_2, as well as that of N and O (left axis, arbitrary units). Comparison with the results of the model (dashed lines, right axis). The theoretical predictions of N are shown for three different dissociation rate constant values, k_{D4} (cm^3s^{-1}). The theoretical predictions of O are also shown for three different sets of dissociation rate constant values k_{D2} and k_{D3} (cm^3s^{-1}), calculated from the formulae of ref [44] for three electron mean energies E_e (eV) (see text). The experimental results have been shifted slightly downwards or upwards for clarity of display. The conditions of the discharge were 0.12 mbar of NO, 1 sccm, 40 mA.

Fig. 5 : Time resolved concentrations of the atomic and molecular species involved in a 0.12 mbar, 1 sccm, 40 mA, NO modulated discharge, as predicted with the present kinetic model.

TABLE I: Reactions included in the kinetics model of the NO hollow cathode discharge. Rate coefficients are in units of cm^3 $molecule^{-1}$ s^{-1} for dissociation by electronic impact and bimolecular reactions; cm^6 $molecule^{-2}$ s^{-1} for trimolecular reactions and s^{-1} for heterogeneous reactions. P is the pressure in mbar.

Reaction	Rate Constant	Reference
Electron Impact Dissociation		
D1 $NO + e \rightarrow N + O(^3P) + e$	8.5×10^{-10}	fit , [22]
D2 $O_2 + e \rightarrow 2\,O(^3P) + e$	6.6×10^{-10}	[44]
D3 $O_2 + e \rightarrow O(^1D) + O(^3P) + e$	3.0×10^{-9}	[44]
D4 $N_2 + e \rightarrow 2N + e$	5.0×10^{-12}	fit, max
D5 $N_2O + e \rightarrow N_2 + O(^3P) + e$	8.0×10^{-10}	fit , [22]
D6 $N_2O + e \rightarrow N_2 + O(^1D) + e$	3.7×10^{-10}	fit , [22]
D7 $N_2O + e \rightarrow NO + N + e$	1.2×10^{-10}	fit , [22]
D8 $NO_2 + e \rightarrow NO + O(^3P) + e$	8.5×10^{-10}	fit , [22]
Quenching of Excited States		
Q1 $O(^1D) + NO \rightarrow O(^3P) + NO$	1.5×10^{-10}	[53]
Q2 $O(^1D) + N_2 \rightarrow O(^3P) + N_2$	2.6×10^{-11}	[53]
Q3 $O(^1D) + O_2 \rightarrow O(^3P) + O_2$	4.0×10^{-11}	[42]
Homogeneous Reactions		
G1 $N + NO \rightarrow N_2 + O(^3P)$	3.0×10^{-11}	[54]
G2 $O(^3P) + NO + M(N_2) \rightarrow NO_2 + M(N_2)$	1.0×10^{-31}	[53]
G3 $O(^3P) + NO_2 \rightarrow NO + O_2$	9.7×10^{-12}	[53]
G4 $N + NO_2 \rightarrow N_2O + O(^3P)$	1.2×10^{-11}	[42]
G5 $O(^1D) + NO \rightarrow O_2 + N$	8.5×10^{-11}	[54]
G6 $O(^1D) + N_2O \rightarrow 2\,NO$	7.2×10^{-11}	[53]
G7 $O(^1D) + N_2O \rightarrow N_2 + O_2$	4.9×10^{-11}	[42]
G8 $O(^1D) + NO_2 \rightarrow NO + O_2$	3.0×10^{-10}	[54]
Heterogeneous reactions		
W1 $O(^3P) + wall \rightarrow O(S)$	4195/P	dif, [20]
W2 $O(^3P) + O(S) \rightarrow O_2$	180	[19,20,45]
W3 $N + wall \rightarrow 1/2\,N_2$	16.1	[19, 45]
W4 $N + O(S) \rightarrow NO$	180	[20]
W5 $NO + O(S) \rightarrow NO_2$	0.06	fit
W6 $N_2 + O(S) \rightarrow N_2O$	0.004	fit
W7 $O(^1D) + wall \rightarrow O(^3P)$	4195/P	dif, [19,55]

max: maximum value
dif: limited by diffusion because of a high sticking or deexcitation probability
fit, [22]: fitted from experimental data, [coincident with previous work on N_2O discharges]

References

[1] Cartry G, Magne L and Cernogora G 1999 *J. Phys. D: Appl. Phys.* **32** 1894-907
[2] Date L, Radouane K, Despax B, Yousfi M, Caquineau H and Hennad A 1999 *J. Phys. D: Appl. Phys.* **32** 1478-88
[3] Guerra V and Loureiro 1997 *Plasma Sources Sci. Technol.* **6** 373-85
[4] Stefanovic I, Bibinov N K, Deryugin A A, Vinogradov I P, Napartovich A P and Wiesemann K 2001 *Plasma Sources Sci. Technol.* **10** 406-16
[5] Sakai Y and Tagashira H 1993 *Non-Thermal Plasma Techniques for Pollution Control* NATO ASI Series Vol. G 34 Part A (Berlín: Springer-Verlag) pp 139-49
[6] Arcos T, Domingo C, Herrero V J, Sanz M M, Shulz A and Tanarro I 1998 *J. Phys. Chem. A* **102**, 6282-91
[7] Nahorny J, Ferreira C M, Gordiets B, Pagnon D, Touzeau M and Vialle M 1995 *J. Phys. D: Appl. Phys.***28** 738-747
[8] Wahl G, Decker W, Klippe L, Nürnberg A, Pulver M and Stolle R 1995 *Conventional and novel chemical vapor deposition techniques - Coating methods to protect materials against hostile environments* Pauleau Y (ed) NATO ASI Series E. **250** (Berlin: Springer) pp 185-244
[9] Tabarés F L, Tafalla D and de la Cal E 1999 *Recent Res. Devel. Vacuum Sci. & Tech.* **1** 93-134
[10] Hsiao M C, Penetrante B M, Merritt B T, Vogtlin G E and Wallman P H 1997 *J. Adv. Oxid. Technol.* **2** 283-5
[11] Mok Y S, Ham S W 1998 *Chem. Eng. Sci.* **53** 1667-78
[12] Baeva M, Gier H, Pott A, Uhlenbusch J, Höschele J and Steinwandel J 2002 *Plasma Sources Sci. Technol.* **11** 1-9
[13] Kossyi I A, Yu Kosstinsky A, Matveyev A A and Silakov V 1992 *Plasma Sources Sci. Tech.* **1** 207-20
[14] Wayne R P 2000 *Chemistry of Atmospheres* (Oxford: Oxford Univ. Press)
[15] Mavrodineau R 1984 *J. Res. Nat. Bur. Standards* **89**, 143-85
[16] Caroli S (ed.) 1985 *Improved Hollow Cathode Lamps for Atomic Spectroscopy* (New York: John Wiley & Sons)
[17] Arslanbekov R R and Kudryavtsev A A 1998 *Proceedings of the NATO Advanced Research Workshop on Electron Kinetics and Applications of Glow Dischargers* NATO ASI Series Book (New York: Plenum) pp 161-178
[18] Tanarro I, Sanz M M, Bermejo D, Domingo C and Santos J 1994 *J. Chem. Phys.* **100** 238-46
[19] Cleland T A and Hess D W 1989 *J. Electrochem. Soc.* **136** 3103-11
[20] Kline L E, Partlow W D, Young R M, Mitchell R R and Congedo T V 1991 *IEEE Transactions on Plasma Science* **19** 278-85
[21] Tanarro I, Arcos T, Domingo C, Herrero V J and Sanz M M 2002 *Vacuum* **64** 457-65
[22] Arcos T, Domingo C, Herrero V J, Sanz M M, Schulz A and Tanarro I 2000 *J. Phys. Chem. A* **104**, 3974-83
[23] Arcos T, Castillo M, Domingo C, Herrero V J, Sanz M M and Tanarro I 2000 *J. Phys. Chem. A* **104**, 8183-93
[24] Tanarro I, Sanz M M, Bermejo D, Domingo C, Santos J and Domenech J L 1994 *J. Phys. Chem.* **98** 5862-66
[25] Behle S, Brockhaus A and Engemann J 2000 *Plasma Sources Sci. Technol.* **9** 57-67
[26] Itatani R 1998 *Plasmas & Ions* **1** 37-44
[27] Schott L 1995 *Plasma Diagnostics* Lochte-Holtgreven W (ed) (New York: AIP Press) pp 668-731

[28] Johnson O and Malter L 1950 *Phys. Rev.***80** 58
[29] Felts J and Lopata E 1987 *J. Vac. Sci. Technol. A* **5** 2273-2275
[30] Laframboise J G 1966 *Institute of Aerospace Studies, University of Toronto, Report No* 100
[31] Allen J E 1995 *Plasma Sources Sci. Techol.* **4** 234-241
[32] Grill A 1994 *Cold Plasma in Materials Fabrication* (New York: IEEE Press)
[33] Clements R M 1978 *J. Vac. Sci. Technol.* **15** 193-198
[34] Arslanbekov R R, Kudryavtsev A A and Tobin R C 1998 *Plasma Sources Sci. Technol.* **7** 310-22
[35] Aroca C, Morón C, López E, Sánchez M C and Sánchez P 1989 *J. Phys. E: Sci. Instrum* **22**, 780-1
[36] Mélen F and Herman M 1992 *J. Phys. Chem. Ref. Data* **21** 831-881
[37] Rothman L S 1992 *J. Quant. Spectrosc. Radiat. Transfer.* **48** 469-507
[38] Harris F J 1978 *Proc IEEE* **66** 51
[39] Striganov A R and Sventitskii N S 1968 *Tables of spectral lines of neutral and ionized atom* (New York: Plenum)
[40] Radzig A A and Smirnov B M 1980 *Reference data of Atoms, Molecules and Ions* (Berlin: Springer-Verlag)
[41] McDaniel E W 1989 *Atomic Collisions, electron & photon projectiles* (New York: John Wiley & Sons)
[42] 1992 *NIST Chemical Kinetics Database* (Gaithersburg: U. S. Department of Comerce)
[43] NASA Panel for Data Evaluation 1997 and 2000 *Chemical Kinetics and Photochemical Data for use in Stratospheric Modeling* JPL Publications 97-4 and 00-3 Evaluation Numbers 12 and 13. http://jpldataeval.jpl.nasa.gov/
[44] Lee C, Graves D B, Lieberman M A and Hess D W 1994 *J. Electrochem. Soc.* **141** 1546-1555
[45] Morgan J E and Schiff H I 1966 *U. S. Gov. Res. Dev. Rep. **5*** 67
[46] Ferreira C M and Gordiets B 1997 *Electron kinetics and applications of glow discharges* Kortshagen U and Tsendin (eds) NATO-ASI SeriesB. **367** (New York: Plenum) pp 391-407
[47] Tserepi A D and Miller T A 1995 *J. Appl. Phys.* **77** 505-511
[48] Adams S F and Miller T A 2000 *Plasma Sources Sci. Technolol.* **9** 248-255.
[49] von Keudell A 2000 *Plasma Sources Sci. technol.* **9** 455-467
[50] Levine I R 1978 *Physical Chemistry* (New York: Mc Graw-Hill) pp 448-449
[51] Hirschfelder J O, Curtiss C F and Bird R B 1954 *Molecular theory of gases and liquids* (New York: John Wiley & Sons) pp 539
[52] Chantry P J 1987 *J Appl Phys* **62** 1141-1148
[53] Atkinson R, Baulch D L, Cox R A, Hampson Jr. R F, Kerr J A, Rossi M J and Troe J 1999 *J. Phys. Chem. Ref. Data* **28** 191-393
[54] Atkinson R, Baulch D L, Cox R A, Hampson Jr. R F, Kerr M J and Troe J 1989 *J. Phys. Chem. Ref. Data* **18** 881-1097
[55] Brake M L and Kerber R L 1983 *Plasma Chem. Plasma Process.* **3** 79

Figures

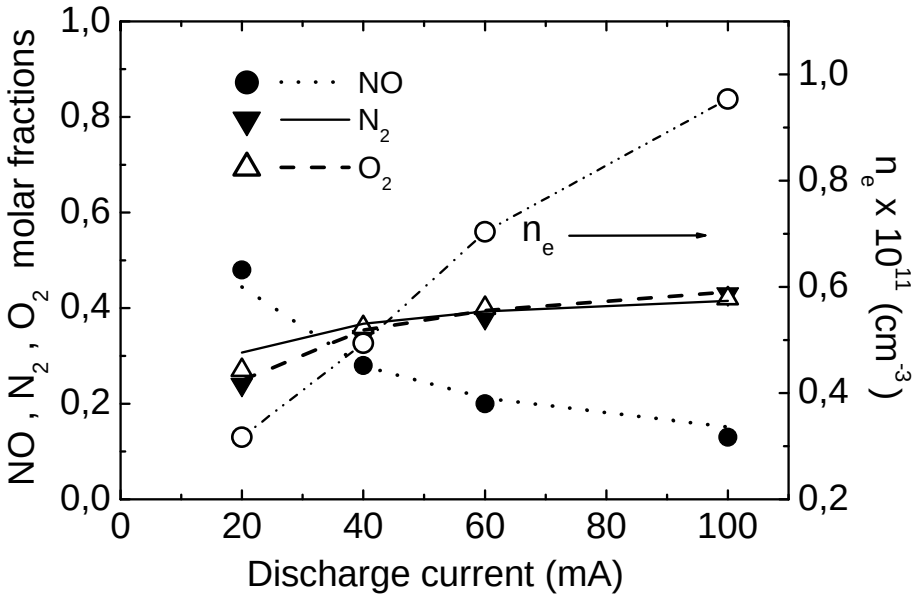

Figure 1

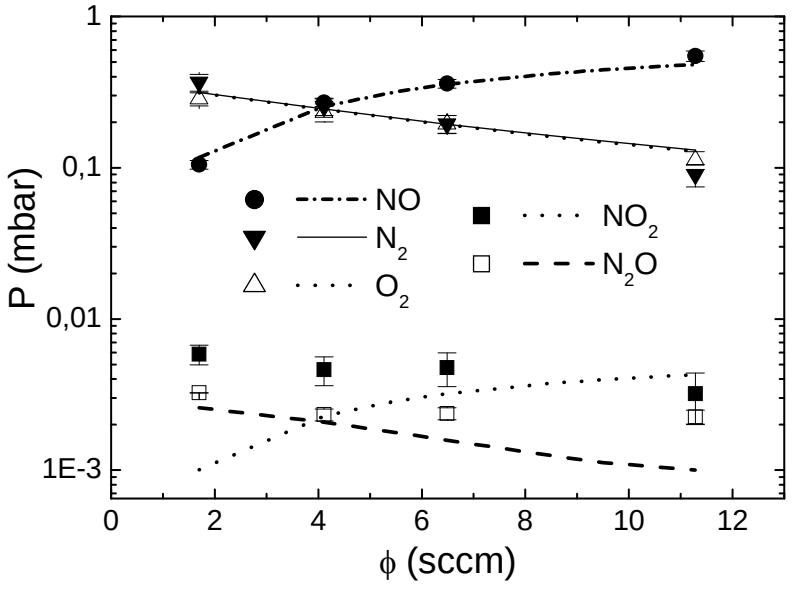

Figure 2

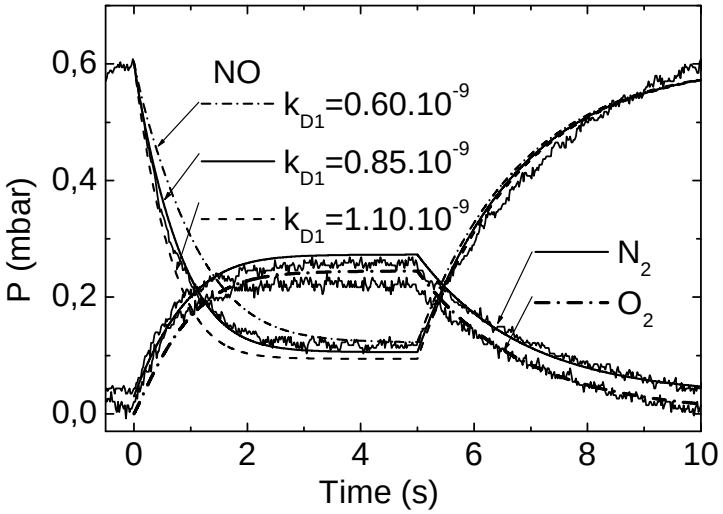

Figure 3

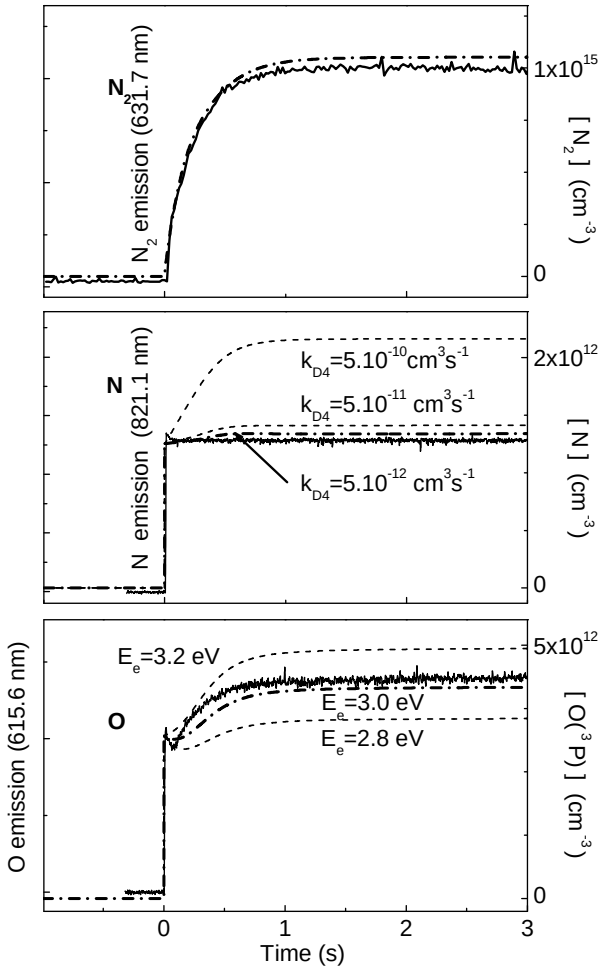

Figure 4

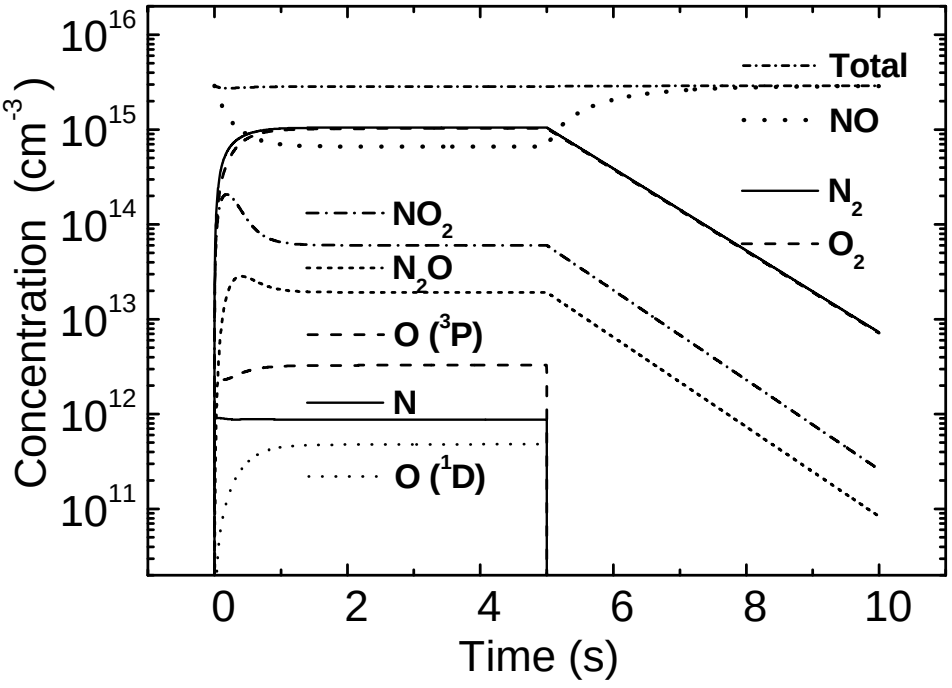
Concentration (cm^{-3})
10^{16}
10^{15}
10^{14}
10^{13}
10^{12}
10^{11}
0
2
4
6
8
10
Time (s)
Total
NO
N_2
O_2
NO_2
N_2O
O (^{3}P)
N
O (^{1}D)

Figure 5